

Aerodynamic Characterisation of Rocket Fin Flutter Using Computational Fluid Dynamics (CFD)

Dr Nnorom Achara, Engr. Bongdap Nanbol Keza

Abstract—In this study a theoretical flutter model has been used in MATLAB to obtain flutter speeds for subsequent use in ANSYS analysis. The geometry of the fin was created in Solid works CAD platform and exported to ANSYS fluent, where input of influence parameters were made and analyzed for aerodynamic pressures. These were then mapped to the structural fin in ANSYS mechanical and the resulting deformations viewed. The aerodynamic behaviors of rocket fin were studied and the results before the flutter speed, at the flutter regime and after the flutter speed were displayed. The aerodynamic pressure is found to be highest at the leading edge and the deformation turns from bending to torsion as the flutter speed increases. The post-critical flutter records the highest displacement. The work also showed the modal analysis of the rocket fin with the natural frequencies which were validated with data from Falcon V launch.

Index Terms—supersonic, rocket stability, clipped delta, leading edge, tropopause

I. INTRODUCTION

Depending on its mission, Rockets are vehicles designed to fly within a certain angular rate of attack at high speeds in the atmosphere and beyond. Mission success depends on flight stability, a major performance consideration. The rocket fins are aerodynamically designed to achieve this flight objective. These fins are subjected to high aerodynamic loads during flight. The understanding and accurate modeling of these aerodynamic characteristics play a major part in their performance. The equations governing the dynamics of these fins in flight are nonlinear partial differential equations which are difficult to model analytically and are expensive or sometimes limited in scope to be solved through wind tunnel experimental studies. Therefore an option most often used by workers in this area is the numerical solution route. Since the rocket fin motion in air is a Fluid-Structure-Interaction (FSI) problem, Computational Fluid Dynamics (CFD) numerical technique is usually adopted in the analysis.

The rockets fins are either passive or active in terms of flight stabilisation and this depends on whether the fins are fixed or movable. The fins are designed to operate stably over a range of speeds, but beyond this range however, the fins begin to vibrate violently to create the flutter

phenomenon. This violent unstable structural vibration appears to originate most often from the coupling of two vibrational modes in the aero elastic system. This vibration is responsible for the extraction of energy from the airstream to the structure and potentially this could lead to catastrophic structural failure [1].

Understandably, quite often, rocket designers, aim to use light materials which at the same time are flexible with the resulting effect of distortion when aerodynamic loads are applied. Aerodynamic loads are essentially due to the geometry of the lifting surface structures. If somehow these loads cause deformations in the structure and vary the geometry, a totally different aerodynamic set of loads will result. These loads would produce increasing distortion in the shape of the lifting surface. The interaction between aerodynamic, elastic and inertia forces is the core subject of aeroelasticity. Various aeroelastic phenomena can be classified by means of Collar's triangle of forces [2]. Three types of forces namely; Aerodynamic forces, Elastic forces, and inertial forces are placed at the vertices of the triangle (see fig. 1). Every aeroelastic phenomenon can be located in relation to the three vertices. Static aeroelastic phenomena due to interaction of aerodynamic and elastic forces (such as lifting surface divergence or control surface efficiency) and dynamic aeroelastic phenomena (such as flutter, dynamic response and buffeting) can easily be located since they involve all the three kinds of forces. The interaction of elastic and inertial forces important for the analytical treatment of dynamic aeroelastic problem gives rise to mechanical vibrations, where as the interaction between the aerodynamic and the inertial forces introduces rigid body dynamics.

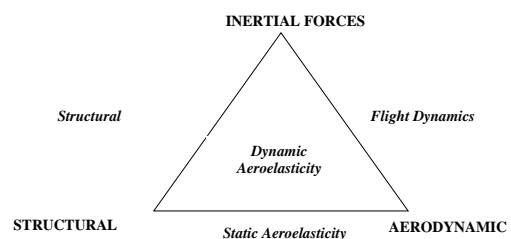


Figure 1 Collar's Triangle of Forces

Flutter characteristics of fins are highly coupled to their aspect ratio, with lower aspect ratios having higher flutter velocities which can be calculated by using equation (i). Fitting fins on rockets help to keep the centre of pressure (C_p) aft of the Centre of gravity (C_g). As long as this condition is maintained, small perturbations in the direction of flight are restored by the aerodynamic forces on the fins.

Though a number of factors contribute to the location of

Dr Nnorom Achara, Mechanical Engineering, Nigerian Defence Academy, Kaduna, Nigeria
Engr Bongdap Nanbol Keza, Mechanical Engineering, Nigerian Defence Academy, Kaduna, Nigeria

the C_p , by far the fin's panel area has the greatest influence. In 1967, James Barrowman derived a set of tools to predict the C_p for a rocket based on the nose cone, body, fin geometries and the Mach number. These tools included a set of equations, the Barrowman Equations, for calculating the C_p at subsonic speeds, and a computer program, called "Fin", to iteratively solve for the C_p at supersonic speeds. [3]

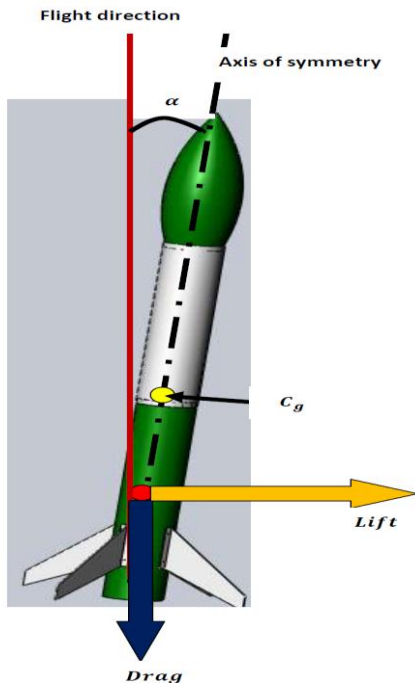


Figure 2 Pictorial representation of typical aerodynamic forces acting on the rocket

Flutter is characterized by the superposition of two structural modes – the pitch and plunge movement. With increasing wind speed, the frequency of these vibration modes coalesce to create the resonance of flutter, i.e. when the pitch frequency and the plunge frequency become equal at a certain velocity called flutter velocity. Fig. 3 depicts a typical displacement-time curve for flutter phenomenon.

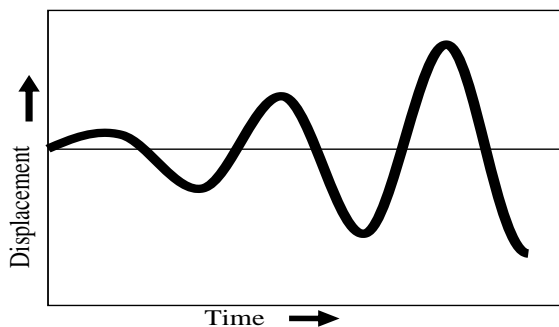


Figure 3 Flutter displacement-time model

Due to the multidisciplinary nature of flutter, a number of factors influence its occurrence and these include Mach number, dynamic pressure, structural stiffness, total mass, mass distribution, system dynamics, and free play [4]. Two criteria are currently used to describe the likely onset of flutter, Flutter velocity V_F and Flutter Dynamic Pressure Q_F . The flutter velocity is the velocity at given flight conditions (Mach number, altitude, etc.) beyond which a small disturbance is very likely to initiate flutter in the component

under inspection. Similarly, flutter dynamic pressure is the dynamic pressure at given flight conditions beyond which a small disturbance is very likely to initiate flutter in the component under consideration.

Joseph R. Simmons, III developed a multidisciplinary design tool that minimizes the mass of the fins while maintaining aerodynamic performance. The tool developed during this research is designed to find an optimal solution for the fin geometry based on the competing needs of minimizing the fins' mass and ensuring the fins will not experience flutter. The design tool therefore provides a means to verify the fin performance throughout the designed flight profile. [5]

The purpose of this work is to use MATLAB and Computational Fluid Dynamics (CFD) to study the phenomenon of rocket fin flutter.

II. EQUATIONS FOR MODELING THE FLUTTER PHENOMENON

By the use of aeroelastic theory, wind tunnel and flight test data, equations estimating flutter velocity has been obtained. One of such equations from APOGEE ROCKET Newsletter is given here as equation (i), [6].

$$V_F = a \sqrt{\frac{G}{\frac{1.337AR^3P(\lambda + 1)}{2(AR + 2)\left(\frac{t}{C_r}\right)^3}}}$$
 (1)

Where, G = Shear modulus of torsion (Pa), b = Half or semi Span (m), t_{max} = Maximum Fin thickness (m)

C_r = Root chord (m), C_t = Tip chord (m), AR = Panel aspect ratio, λ = Taper ratio, C_{av} = Average chord (m) with atmospheric influence equations given as follows:

a. Temperature

$$T_h = T_0 - \frac{6.5h}{1000}$$
 (2)

b. Pressure

$$p_h = p_0 \left(1 - 0.0065 \frac{h}{T_0}\right)^{5.2561}$$
 (3)

c. Speed of sound

$$a = a_0 + 0.606 \times \left(\frac{5}{9}(T - 32)\right)$$
 (4)

The relevant initial constants needed for the atmospheric influence calculations include pressure, temperature, sonic speed which are respectively $101325 N/m^2$, $288.15 K$, $331.3 m/s$.

The equations governing the general fluid motion are derived from the three fundamental principles of mass, momentum, and energy conservation.

It is assumed that the fluid (air) is Newtonian, incompressible and that viscosity is constant at the fin surface but inviscid farfield. Therefore, the continuity and

Navier-stokes equations as given below are sufficient to model the flow of high speed rocket fin through the fluid:

Continuity Equation:

$$\frac{\partial \rho}{\partial t} + \frac{\partial}{\partial x}(\rho u) + \frac{\partial}{\partial y}(\rho v) + \frac{\partial}{\partial z}(\rho w) = 0 \quad (5)$$

X-Momentum:

$$\rho g_x - \frac{\partial p}{\partial x} + \mu \left(\frac{\partial^2 u}{\partial x^2} + \frac{\partial^2 u}{\partial y^2} + \frac{\partial^2 u}{\partial z^2} \right) = \rho \left(\frac{\partial u}{\partial t} + u \frac{\partial u}{\partial x} + v \frac{\partial u}{\partial y} + w \frac{\partial u}{\partial z} \right) \quad (6)$$

Y-Momentum:

$$\rho g_y - \frac{\partial p}{\partial y} + \mu \left(\frac{\partial^2 v}{\partial x^2} + \frac{\partial^2 v}{\partial y^2} + \frac{\partial^2 v}{\partial z^2} \right) = \rho \left(\frac{\partial v}{\partial t} + u \frac{\partial v}{\partial x} + v \frac{\partial v}{\partial y} + w \frac{\partial v}{\partial z} \right) \quad (7)$$

Z-Momentum:

$$\rho g_z - \frac{\partial p}{\partial z} + \mu \left(\frac{\partial^2 w}{\partial x^2} + \frac{\partial^2 w}{\partial y^2} + \frac{\partial^2 w}{\partial z^2} \right) = \rho \left(\frac{\partial w}{\partial t} + u \frac{\partial w}{\partial x} + v \frac{\partial w}{\partial y} + w \frac{\partial w}{\partial z} \right) \quad (8)$$

Where, ρ = fluid density, p = pressure, t = time, V = fluid velocity.

The primary design parameters useful for the modeling are the root chord C_r , tip chord C_t , the semi-span b i.e. the span of a single fin and the entire span will be $2b$, the sweep angle (φ), and the maximum airfoil fin thickness t_{max} . These parameters are shown in fig. 4.

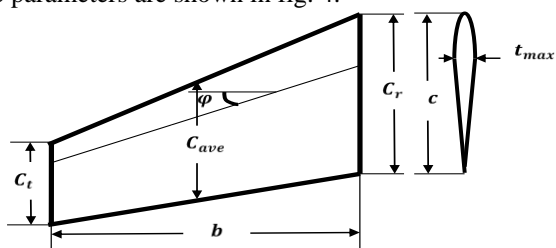


Figure 4 Rocket Fin Design Parameters

An efficient “clipped delta” fin typically has a “fin root cord length” equal (or roughly equal) to its “semi-span length”. The “fin tip cord length” is typically half the “root cord length”. [7]

The derived Design Parameters are; Aspect ratio (AR), Average Chord (C_{ave}), Taper Ratio (λ) and Panel Area (S) mathematically expressed as follows.

$$AR = b/C_{ave} \quad (9)$$

$$C_{ave} = C_r + C_t/2 \quad (10)$$

$$\lambda = C_t/C_r \quad (11)$$

$$S = (C_r + C_t)b/2 \quad (12)$$

NACA-4 digit Airfoil Fin: The most basic requirement for modeling rocket fin aerofoils is that the cross sections must be as symmetrical as possible. This is necessary so that no lift forces are generated when the rocket is at zero angle of attack (in other words, if our model rocket is flying straight, we don't want the fins providing any side forces that may cause the rocket to spin and/or deviate from its course). [8] The aerofoil shaped fin helps reduce both pressure and induced drags. The best rocket fin aerofoil is the **NACA 4-Digit series**, with good stall characteristics, small center of pressure movement across large speed range and roughness has little effect. The symmetrical form of this series (NACA 00xx) is preferred for missiles and rocket fins (see Fig. 5).

The equation for a symmetrical NACA 4-Digit airfoil with a closed trailing edge

$$y = 5T \left(0.2969 \sqrt{x} - 0.1260 x - 0.3516 x^2 + 0.2843 x^3 - 0.1036 x^4 \right) \quad (13)$$

Where: x is the position along the chord from 0 to 1, (0 to 100%)

y is the half thickness at a given value of x (centerline to surface), and

T is the maximum thickness as a fraction of the chord (so t gives the last two digits in the NACA 4-digit denomination divided by 100). The coordinates (x_U, y_U) of the upper airfoil surface and (x_L, y_L) of the lower airfoil surface are

$$x_U = x_L = x, \quad y_U = +y \quad \text{and} \quad y_L = -y$$

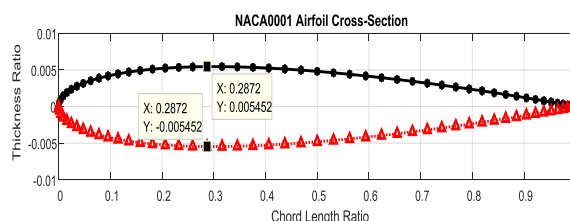


Figure 5 NACA 0001 Airfoil Cross Section

Geometrical model of the fin: The fin studied in this work, is the low speed (subsonic) rocket fin made from NACA0001 airfoil with a Clipped Delta planform shape, created in Solidworks, having the dimensions indicated in mm.

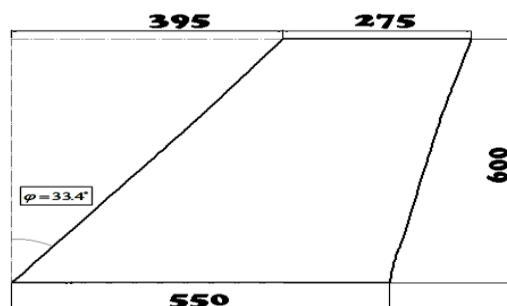


Figure 6 Solidworks model of the Air foiled Rocket Fin Some other parametric values used in this study are shown in table 1.

Table 1 Geometrical and Calculated Data of the fin

Geometric Parameters	Value(mm)	Value(SI)
C_r	550	550
C_t	275	275
b	600	600
t_{max}	6	6
φ	33.4°	33.4°
Calculated parameter	Value (Others)	Value (SI)
S	247500 mm ²	0.25 m ²
AR	1.46	1.46
λ	0.50	0.50

III. TOOLS, MATERIALS AND METHOD

The tools and materials:The tools and materials used in this study include ANSYS SOFTWARE Workbench 18.2, MATLAB R2012b, Solid Works Premium 2013 x64 Edition, Aluminum 1060 alloy and FLUID (Air).

Modeling Methodology: Using, the NACA 4 Digit mathematical model, the rocket fin has been considered as a simple cantilever beam, modeled in Solidworks CAD software and analyzed appropriately. In the modeling, basic properties of fin material as well as atmospheric variables have been considered. MATLAB has been used to obtain flutter speeds and the ANSYS workbench through a system coupling of Static Structural and Fluid Flow (Fluent) toolboxes used to analyze the fin and the air domain. Finally, the flow patterns and dynamic characteristics around the rocket fin are visualized using ANSYS fluent Post Processing window.

IV. RESULT AND DISCUSSION

The analysis in ANSYS is carried out in phases since; the physics is a coupling of two systems- Transient Structural and Fluid Flow (Fluent).

The solution shown below uses equation (i) with a variable maximum airfoil thickness ranging between 6 and 24mm for an Aluminium 1060 alloy of Shear modulus $G = 2.7 \times 10^{10} (Pa)$

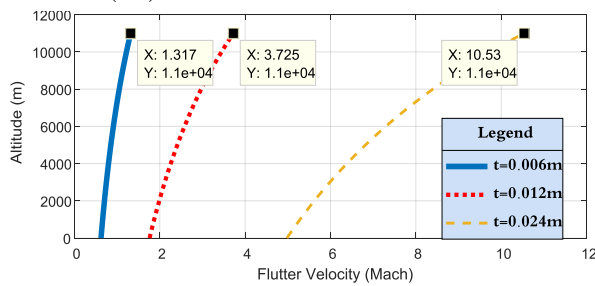


Figure 7 Variation of airfoiled fin maximum thickness with Mach Flutter speed

The maximum flutter speed for the 6mm fin material has been used to set a range of velocities used in the CFD analysis thus 1.3M which corresponds to $(391.2 \pm 100) m/s$ is employed.

The Finite Element mesh consisted of 10470 nodes and 4866 elements with fine Angle span.

The first three mode shapes of Aluminium 1060 NACA0001 airfoil fin are presented below in smooth contours with the undeformed wireframe and their respective frequencies.

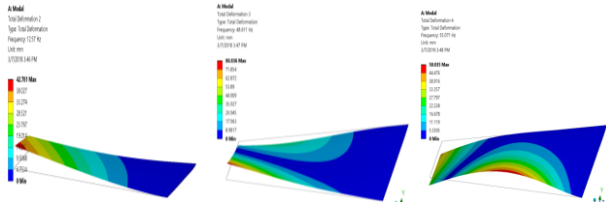


Figure 8(a) 1st mode shape (b) 2nd mode shape (c) 3rd mode shape

The resulting total deformation and stress contours for the three cases – pre-critical, critical and post critical are shown in figures 9, 10 and 11 respectively. Also in table 2, the important parameters predicted for the three cases are shown.

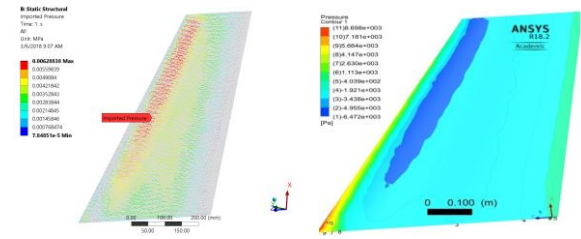
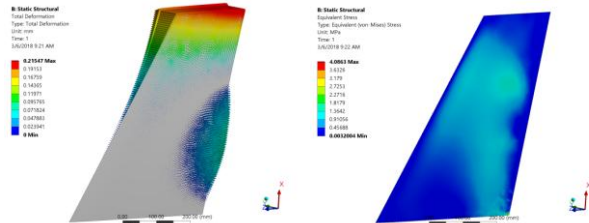


Figure 9 (a) Imported Pressure Load (b) Contours of Aerodynamic Pressure on the Fin



(c) Plots of Total deformation (d) Contours of stress on the Fin

The contours of imported pressure, aerodynamic pressure generated on the fin, total deformation and stress on the fin can be seen in figure 9-11. The figures are plotted with colored legends as a measure of the intensity or magnitude from the least with blue color to the highest in red color. The result in figure 9(b) shows that aerodynamic pressures are high at the fin’s leading edge because it faces the wind directly and has small surface area. Figure 9(c) before the critical flutter speed, shows that the tip chord has highest deformations in bending compared with figures 10a and 11a. This deformation later transforms into torsion within the fin planform area as the flutter speed exceeds the critical value figure 11a.

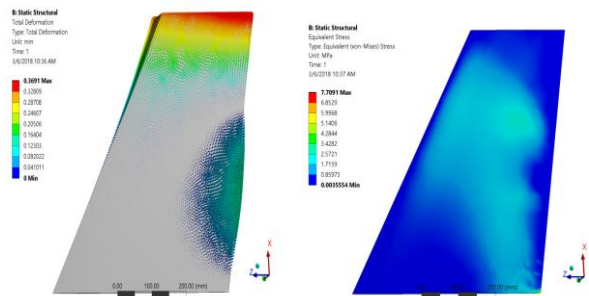


Figure 10 (a) Total deformation (b) Contours of (Von Mises) stress Case C; Post Critical flutter speed Velocity $(491.2 m/s)$

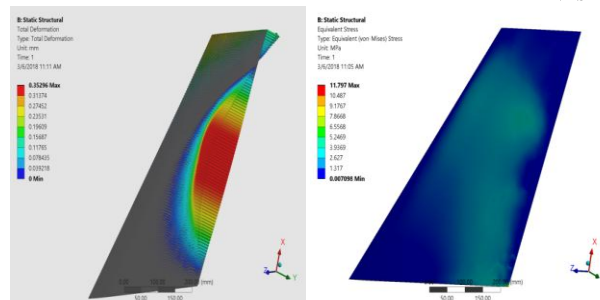


Figure11 (a) Total deformation (b) Contours of Equivalent (Von Mises) stress

Table 2 Summary of Pre, At, and Post Critical Speeds Maximum Results

PARAMETERS	MAXIMUM VALUE		
	Pre-Critical Speed	At-Critical Speed	Post-Critical Speed
Imported Pressure	6.29E-3MPa	1.16E-2MPa	1.82E-2MPa
Velocity	3.16E2m/s	4.25E2m/s	5.37E2m/s
Aerodynamic Pressure	8.70E3Pa	1.52E4Pa	2.45E4Pa
Stress	4.09Mpa	7.71Mpa	11.80Mpa
Deformation	0.2154mm	0.3691mm	0.3596mm

[2] Collar, A. R. "The expanding domain of aeroelasticity". Journal of the Royal Aeronautical Society, vol. 50. pp. 613-636, 1946.

[3] Joseph R. Simmons, III "Aeroelastic Optimization of Sounding Rocket Fins" Air Force Institute of Technology, Wright Patterson Air Force Base, Ohio; United States. pp. 8, June, 2009

[4] NASA space vehicle design criteria: Flutter, buzz, and divergence. Technical Report NASA SP 8003, NASA, 1964. Pp. 1

[5] Joseph R. Simmons, III "Aeroelastic Optimization of Sounding Rocket Fins" Air Force Institute of Technology, Wright Patterson Air Force Base, Ohio; United States. pp. IV, 2009

[6] Zachary Howard, How To Calculate Fin Flutter Speed. PEEK OF FLIGHT Apogee Rocket Newsletter, ISSUE 291, pp 2, July 19, 2011.

[7] Bart Hennin, Peak of Flight News letter. Issue 305 pp. 6, 7, January 31, 2012

[8] Joseph R. Simmons, III "Aeroelastic Optimization of Sounding Rocket Fins" Air Force Institute of Technology, Wright Patterson Air Force Base, Ohio; United States. pp. 55, June, 2009

The flutter growth is shown in figure 12 for the three cases considered and it is clearly shown that the post critical torsional displacement is the highest.

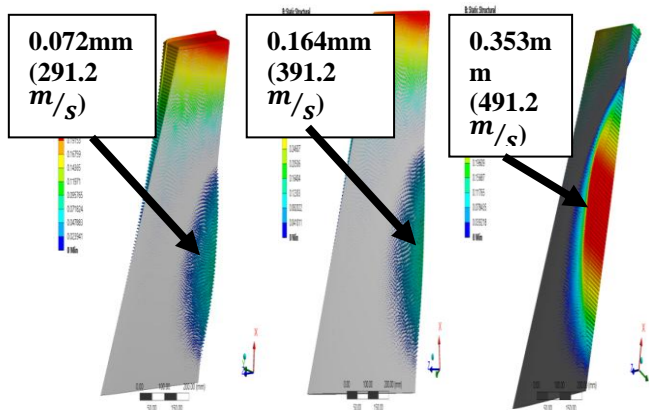


Figure 12 Flutter growth depicted

Although the result of the modal frequency is not shown here, literature data from the ANSYS software compared with Falcon V launch under similar parametric conditions shows a fairly good agreement. [9]

V. CONCLUSION

The flutter of a rocket fin has been studied and it has been found that aerodynamic pressure is highest at the leading edge of the fin and that the tip chord has the highest bending deformations before the critical flutter speed but after the critical speed transforms into torsional deformation whose displacement ranged from 0.072mm for the pre-critical to 0.353mm for the post-critical.

ACKNOWLEDGMENT

The authors wishes to acknowledge the Nigerian Defence Academy for providing an enabling environment and facilities for research. Engr Bongdap Nanbol Keza thanks the Petroleum Technology Development Fund a parastatal of the Federal Government of Nigeria for providing research fund.

REFERENCES

[1] Sebastian Timme, Computational Fluid Dynamics applied to Transonic Aeroelastic Instability Searches CFD Laboratory, University of Liverpool, Liverpool L63 3GH, United Kingdom. pp. 1.